Environmental Science & Technology Letters

pubs.acs.org/journal/estlcu

Letter

Membrane Charge Weakly Affects Ion Transport in Reverse Osmosis

Mikhail Stolov and Viatcheslav Freger*

Cite This: *Environ. Sci. Technol. Lett.* 2020, 7, 440−445

Read Online

ACCESS | Metrics & More | Article Recommendations | Supporting Information

ABSTRACT: Polyamide reverse osmosis (RO) membranes have been a "golden standard" in water desalination, with an aromatic polyamide layer providing an excellent balance between salt rejection and water permeability. Yet, there still are gaps in understanding the salt transport in RO, closely related to the nature and formation of membrane charge and its effect on ion permeation. We report here a systematic investigation that examines the correlation between the nominal membrane charge, determined by ion-binding methods, and key ion permeation characteristics, salt permeability, and membrane conductivity, at different pH values. In the mid-pH range, the most important in the desalination practice, observed relations between the conductivity, salt permeability and nominal charge show a much weaker dependence than the Donnan model predicts. This indicates that fixed charged groups inside polyamide films are largely deactivated, thereby the membrane behaves as effectively neutral or weakly charged. However, a substantial charge may form at extreme acidic and basic pH via uptake of H^+ and OH^- ions, which increases ion uptake and conductivity, promoting polymer swelling and weakening salt rejection. Overall, the results strongly suggest that fixed charges weakly affect salt rejection in RO, and it is dominated by dielectric and steric mechanisms.

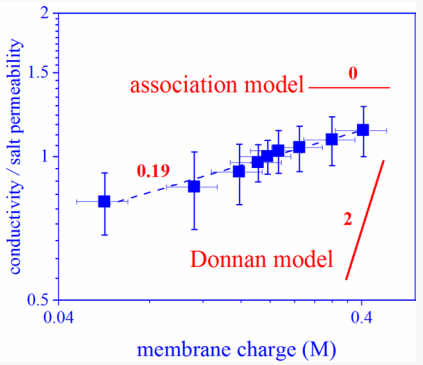

INTRODUCTION

Polyamide thin-film composite reverse osmosis (RO) membranes show excellent removal of salts along with good water permeability.[1] Their good performance is due to a thin barrier layer of aromatic or semiaromatic polyamide;[2] however, the exact selectivity mechanism is still incompletely understood. For instance, its high rejection of salts stands in contrast with a moderate rejection of similarly sized uncharged solutes such as boric acid.[3] Further development motivates better understanding of ion and molecular transport.

For several decades, the standard theoretical framework has been the generalized Donnan model, combining steric, Donnan, and dielectric exclusion in a mean-field manner (SDE model).[4−8] However, inconsistencies regarding the observed effects of pH,[9] ion type and charge,[10] and solution composition[11] on salt permeation pose questions. Recently, we pointed out that inconsistencies may be removed by including *charge-regulation via ion association*.[12,13]

Recently, significant progress was achieved in assessing polyamide fixed charge density, a key characteristic originating from carboxylic and amine groups remaining unreacted after interfacial synthesis.[8,14,15] Their content was eventually measured using ion-exchange,[16] Rutherford backscattering spectrometry (RBS),[17,18] quartz crystal microbalance (QCM),[19] liquid scintillation, and visible light spectroscopy.[20] They indicate that the polyamide charge is pH dependent and negative down to about pH 3, consistent with zeta potential measurements.[21−24] However, our recent analysis shows that the *nominal* chemical charge, assessed by the above ion-binding methods, may have a weaker relation to ion transport due to formation of associates. The resulting *effective* charge becomes smaller and unrelated to the nominal one;[12,13] the present study aims to elucidate these recent findings.

Our approach is based on comparing two complementary ion transport characteristics of polyamide membranes: salt permeability, deducible from filtration experiments, and conductivity, measured here using electrochemical impedance spectroscopy (EIS).[25−27] They are related in a different way to the permeabilities of co-ions and counterions, i.e., anions and cations in the case of polyamide. Within the SDE models, the conductivity is determined mostly by counterion permeability, approximately proportional to the fixed charge density X. Conversely, salt permeability is controlled by co-ion permeability, inversely related to X. The ratio of the two is then expected to vary approximately as X^2. In contrast, the association model anticipates that the ratio will be weakly dependent on X.[13] A similar situation is expected when only a small uncharged fraction of the membrane controls the ion permeation,[12] unrelated to X measured for the entire film. The known dependence of X on pH for polyamide membranes,

Received: April 10, 2020
Revised: April 29, 2020
Accepted: April 30, 2020
Published: April 30, 2020

https://dx.doi.org/10.1021/acs.estlett.0c00291
Environ. Sci. Technol. Lett. 2020, 7, 440−445

made available by RBS,[17,18] offers a straightforward way to test these relations.

MATERIALS AND METHODS

Chemicals and Materials. NaCl, NaOH, and HCl (AR grade) were obtained from Bio-Lab Chemicals. Ultrapure water (UPW, 18.2 MOhm cm) was used for preparing solutions. A SWC4B composite PA membrane was supplied by Hydranautics.

EIS. EIS setup was described in detail previously.[27−29] Briefly, polyamide film isolated from the SWC4B membrane coated a rotating disk working electrode (WE) immersed in a 50 mL glass electrochemical cell containing also a Pt foil (counter electrode, CE) and Ag/AgCl/KCl reference electrode (RE) and was then purged with N_2 (Supporting Information). The cell was filled with a 1 M NaCl solution adjusted to the desired pH with NaOH or HCl, which negligibly affected solution conductivity. High NaCl concentration, close to seawater, was preferred for differentiating film resistance from solution resistance.[27]

EIS spectra were recorded on SP-300 potentiostat (Bio-Logic) in the pH range from 1.5 to 12.4. Spectra were collected every 1 min for 3 to 24 h until membrane resistance stabilized and then were fitted to an equivalent circuit[30] to yield transmembrane resistance R_m and conductivity $G_m = 1/R_m$. Long stabilization could also relax the film and eliminate temporary enhancement of permeability by support-removing solvent;[31] thus, isolated films reasonably represented barrier properties of the polyamide.[32−34] Each point in the EIS spectra was the average of three measurements for each film, with all films showing similar variation of G_m with pH. To address sample variability, G_m values for each film at different pH values were normalized to G_m at pH 7 (Supporting Information).

Filtration Experiments. Membrane sheets were annealed in a NaCl solution of pH 2 that was heated to 30 °C for 5−10 min and then let to cool to room temperature overnight. Flux and NaCl passage in the pH range from 2 to 11 were measured using the setup described previously[10,35] (Supporting Information). Briefly, 4 L of 32 g/L NaCl solution maintained at 298 K was circulated with a high-pressure pump through two identical flow cells at a pressure of 43 bar and a feed flow rate of 130 L/h (average velocity in the channel 0.82 m/s). For each pH, a fresh NaCl solution adjusted to the desired pH was used. Feed was circulated for at least 1 h before collecting permeate. Volume flux was measured by weighing permeate. Salt concentrations were determined from solution conductivity; for pH < 4 chloride was titrated (751 GPD Titrino, Metrohm) to address H^+ conduction. The feed concentration was corrected for concentration polarization (CP) as follows

$$c' = (c_F - c'')\exp\left(\frac{J_V}{k_d}\right) + c'' \quad (1)$$

where c_F, c', and c'' are the feed, CP-corrected feed, and permeate concentrations; J_V is the volume flux, and $k_d = 33$ μm/s is the mass transfer coefficient for the present cell.[36] The salt permeability ω_s was then calculated as follows

$$\omega_s = J_V \frac{c''}{c' - c''} \quad (2)$$

RESULTS AND DISCUSSION

Effect of pH on Membrane Conductivity. Figure 1a shows average variation of membrane conductivity with pH

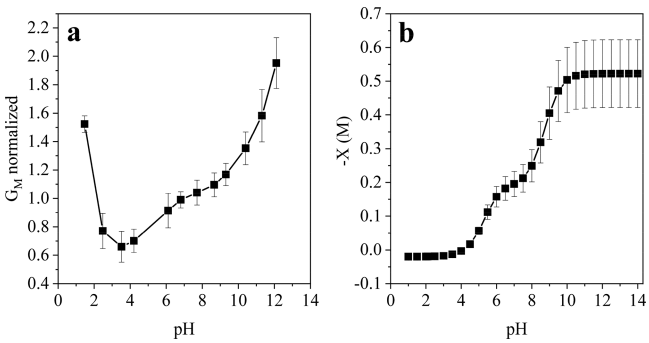

Figure 1. Dependence on pH of (a) polyamide film conductivity normalized to conductivity at pH 7 (this work) and (b) nominal fixed membrane charge. In panel (a), points represent average conductivity normalized to pH 7 for each film, when necessary interpolated to the given pH. Results in panel (b) represent the average ion-binding capacity of four fully aromatic polyamide membranes FT 30, LF 30, TFC-S, and ESNA reported by Coronell et al.[18] (Supporting Information). Error bars show standard deviations.

normalized to pH 7. The trend closely resembles the change in the nominal charge X by RBS reported by Coronell et al.[17,18] (Figure 1b), especially in the middle pH range from 4 to 9. However, a few points are notable. First, conductivity varies far more moderately than X. Thus, conductivity barely doubles between pH 4 and 7, while X increases many times, from nearly zero to about 0.1 M. Similarly, between pH 7 and 10 conductivity increases by ∼50%, whereas the X increase is nearly 3-fold. The conductivity then does not vary proportionally to X, as is typical for well-hydrated homogeneous charged polymers, e.g., ion-exchange membranes.[37,38]

Second, at pH < 4, the conductivity sharply increases. RBS data indicate a small positive charge, <0.05 M, in this pH range, assigned to unreacted amino groups.[17] However, it is small and unlikely to produce a 2-fold increase in conductivity at pH 2, about equivalent to conductivity at pH 9, where $X \sim$ 0.5 M is negative and much larger (Figure 1b). We presume that this upturn in conductivity is best explained by the enhanced uptake of protons. Our recent studies[29,39] indicate that polyamide has a large affinity to protons, about 10^3 times larger than to Na^+ ions. For the 1 M NaCl concentration used here, protons should overtake Na^+ at pH 3, which is consistent with results in Figure 1a.

Finally, conductivity does not level off and continues to increase at pH > 9, despite X staying constant. Uptake of OH^- ions may explain this behavior, similar to proton uptake at low pH. Another reason may be enhanced swelling, increasing ion mobility[40] and fixed charge dissociation, which may increase conductivity at a constant X. However, such increased swelling is again most reasonably explained by the uptake of OH^- ions. Larger swelling also increases the dielectric constant of the membrane, weakening dielectric exclusion of co-ions. This may affect salt permeability and passage more than conductivity, as discussed next.

Effect of pH on Volume Flux and Salt Passage. Figure 2 displays the present results on water flux and salt passage at different pH values along with some literature data[41,42] for aromatic polyamide membranes. The literature data employed

https://dx.doi.org/10.1021/acs.estlett.0c00291
Environ. Sci. Technol. Lett. 2020, 7, 440−445

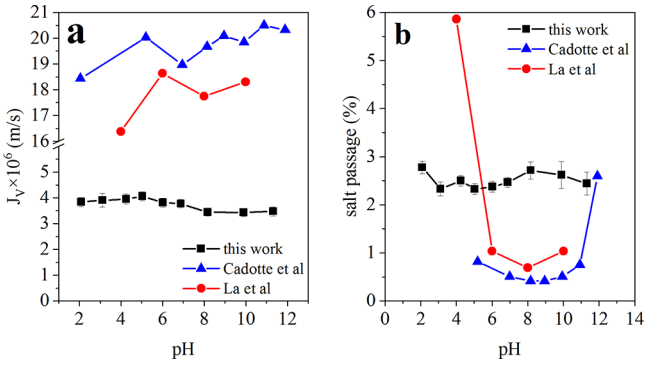

Figure 2. Measured volume flux (a) and NaCl passage (b) as a function of feed pH, obtained in this work and those reported by La et al.[41] and Cadotte et al.[42] Error bars are standard deviations.

much lower salt concentrations of 2 and 5 g/L, as compared to 32 g/L in this work and are used here for comparing the observed trends.

It is well seen that the flux variations with pH are small, not showing any well-pronounced trend. Similar to NF membranes,[43−45] we observed that, at room temperature, varying pH produced scattered results, depending on the direction of pH variations, that we attributed to slow polyamide relaxation, especially toward acidic pH, where polyamide should be most shrunken and relax more slowly. Therefore, we carefully preconditioned membranes in a feed solution at pH 2 and performed tests in the order of increasing pH with at least an hour stabilization at each tested pH. With these precautions, we obtained no significant variation of the membrane permeability with pH, consistent with other data shown.

On the other hand, for the previously reported low-salinity feeds, variation of salt passage with pH in Figure 2b shows a clear minimum around pH 8 and increases toward both acidic and alkaline conditions. If dissociation of carboxylic (at high pH) or amine groups (at low pH) increased the effective membrane charge, the Donnan mechanism would suppress salt passage, opposite to what is observed. We then assign increased salt passage to increased swelling of the membrane induced by uptake of H^+ and OH^- ions, as conductivity data suggest. Although such uptake is also equivalent to increasing membrane charge, which should suppress salt passage, swelling promoted by higher ion content weakens dielectric exclusion and increases ion mobility, which may well offset the increased charge.

Surprisingly, the present results for salt passage in Figure 2b do not show any significant variation with pH. We explain this by higher feed salinity producing osmotic and/or charge-screening-driven deswelling. Salinity-induced deswelling is well known for semiaromatic membranes[46] and well correlates with their reduced permeability for high-salinity feeds.[45,46] Yet, aromatic polyamides are more rigid and have lower swelling,[46−49] and, although they still respond to salinity and pH, the response is weaker. Deswelling makes the response even more sluggish, which may explain the weak effect of pH on flux and salt passage observed here.

Conductivity-to-Salt Permeability Ratio. The weak correlation between salt passage and *nominal* fixed charge (as measured by RBS) suggests the latter may not be identified as the *effective* charge of the polyamide or its part that rejects salt. This point is best analyzed by considering the ratio of the membrane conductivity G_m and salt permeability ω_s (estimated using eq 2), which is the most sensitive indicator of the effect of charge on ion transport. Indeed, G_m and ω_s have the following relations to individual ion permeabilities ω_+ and ω_-[30,50]

$$G_m = \frac{F^2 A}{RT}\sum_i C_i\omega_i \approx \frac{F^2 A}{RT}C_s(\omega_+ + \omega_-) \tag{3}$$

$$\omega_s = \frac{2}{\omega_+^{-1} + \omega_-^{-1}} \tag{4}$$

where ionic permeabilities (i = + or −) are understood as[29]

$$\omega_i = \frac{D_i S_i}{\delta} \tag{5}$$

and A and δ are the polyamide film area and thickness, C_i, D_i, and S_i are the solution concentration, diffusivity in the membrane, and sorption coefficient (membrane/solution partitioning) of the ion, respectively, and F, R, and T are Faraday constant, gas constant and temperature, respectively. The last relation in eq 3 implies that only salt ions contribute to conductivity, which apparently applies here in the range 5 < pH < 9. When constant prefactors (film geometry, solution concentration, thermodynamic constants, etc.) are lumped together, both absolute and normalized G_m/ω_s becomes proportional to the following combination of ion permeabilities

$$\frac{G_m}{\omega_s} \propto (\omega_+ + \omega_-)(\omega_+^{-1} + \omega_-^{-1}) \tag{6}$$

The scaling with membrane charge X may be derived from this relation for different models. For instance, Donnan-based models under strong co-ion (anions here) exclusion predict $S_+ \approx X/C_s$, $S_- \propto 1/S_+ \propto C_s/X$, and X-independent ion diffusivities, which yields

$$(\omega_+ + \omega_-)(\omega_+^{-1} + \omega_-^{-1}) \approx \omega_+\omega_-^{-1} = \frac{D_+S_+}{D_-S_-} \propto X^2 \tag{7}$$

Conversely, our recent model[13] predicts that, under strong charge regulation via association, sorption coefficients, controlled by association equilibria, will be unrelated to X, yet diffusivities will scale as inverse distance between fixed charges, i.e., $X^{-1/3}$. However, since both ion diffusivities show the same scaling, X will cancel out in eq 8 and, ultimately, we expect $G_m/\omega_s \propto X^0$.

The above relations are examined in Figure 3a that plots normalized G_m/ω_s measured for 5 < pH < 9 versus X based on data by Coronell et al.[18] The logarithmic slope (exponent) 0.19 ± 0.01 is clearly much smaller than the value 2 expected for the Donnan model and far closer to 0, predicted for strong association. We then conclude that the total ion-binding capacity of the membrane has only a minor effect on ion permeation.

To complete the picture, Figure 3b also plots the ratio G_m/ω_s directly versus pH in the entire examined pH range, which tests the possible effect of H^+ and OH^- uptake, as an alternative charge formation mechanism, studied previously.[29,39] Considering proton uptake at low pH, the limiting regime of proton-dominated ion uptake leads to the following scaling[29,39]

$$S_- \propto (10^{-\mathrm{pH}}/C_s)^{1/2},\ S_+ \propto 1/S_- \propto (10^{-\mathrm{pH}}/C_s)^{-1/2} \tag{8}$$

https://dx.doi.org/10.1021/acs.estlett.0c00291
Environ. Sci. Technol. Lett. 2020, 7, 440−445

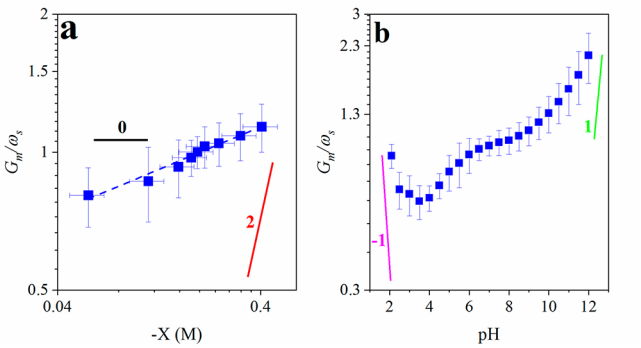

Figure 3. (a) G_m/w_s ratio versus nominal membrane charge X for pH 5 to 9. The values of X are as reported by Coronell el al.[18] Theoretical slopes refer to the Donnan model (2) and association model (0); (b) G_m/w_s ratio versus pH. Shown theoretical slopes correspond to a neutral membrane with cation uptake dominated by H^+ (−1) and anion uptake dominated by OH^- (1). Error bars indicate standard deviation.

Assuming constant diffusivities for mobile ions, the ratio G_m/ω_s will scale with pH approximately as (note anions become counterions)

$$\frac{G_m}{\omega_s} \propto \frac{S_-}{S_+} \propto 10^{-pH} \tag{9}$$

i.e., a linear dependence with an asymptotic slope −1, when G_m/ω_s is plotted on a log scale versus pH. Analogously, in case OH^- uptake dominates charge formation at high pH, the limiting relation becomes

$$\frac{G_m}{\omega_s} \propto \frac{S_+}{S_-} \propto 10^{-pOH} \propto 10^{pH} \tag{10}$$

i.e., the asymptotic slope is +1. Indeed, while pH has no significant effect in middle range, the dependence in Figure 3b seems to transition to the asymptotic regimes defined by eqs 9 and 10 in both extreme pH ranges.

In summary, we see that the Donnan-based picture of ion exclusion cannot describe the relation between ion permeation and the nominal charge, measured by ion-binding methods such as RBS. Apparently, most ion-binding fixed charges are deactivated by association or, in case the membrane is not homogeneous, the charges do not affect the regions controlling salt rejection. On the other hand, H^+ and OH^- ions present in water do affect and enhance ion permeation in extreme acidic and alkaline pH ranges, directly increasing the membrane conductivity. Indirectly, this may also enhance swelling and weaken dielectric exclusion, resulting in a higher salt passage when pH grows very acidic or basic. The latter effect explains the results of previous reports that employed low salinity feeds. However, it was not observed in the present study, presumably, due to membrane deswelling induced by high feed salinity.

Overall, the results strongly indicate that salt rejection in polyamide RO membranes, especially, in the most important mid-pH range, is not or is only weakly controlled by the nominal charge. This agrees with earlier observations for NF membranes[51] and our recent EIS studies of the effect of salinity and salt type.[29,39] It is then most reasonable to view polyamide membranes as effectively neutral or very weakly charged dense polymer films, with salt rejection dominated by dielectric and steric exclusion.

■ ASSOCIATED CONTENT

Supporting Information

The Supporting Information is available free of charge at https://pubs.acs.org/doi/10.1021/acs.estlett.0c00291.

Setups for EIS and filtration experiments, experimental data on membrane conductivity, flux and salt passage, and compilation of membrane charge data (PDF)

■ AUTHOR INFORMATION

Corresponding Author

Viatcheslav Freger − *Wolfson Department of Chemical Engineering, Grand Water Research Institute, and Grand Technion Energy Program, Technion − IIT, Haifa 32000, Israel;* orcid.org/0000-0001-8067-052X; Email: vfreger@technion.ac.il

Author

Mikhail Stolov − *Wolfson Department of Chemical Engineering, Technion − IIT, Haifa 32000, Israel*

Complete contact information is available at: https://pubs.acs.org/10.1021/acs.estlett.0c00291

Notes

The authors declare no competing financial interest.

■ ACKNOWLEDGMENTS

M.S. acknowledges the support by the Center for Absorption in Science of the Israel Ministry of Immigrant Absorption. The financial support by the Israeli Ministry of Energy, VATAT, and the Fuel Choices and Smart Mobility Initiative in the Israeli Prime Minister's Office within the Israeli National Center for Electrochemical Propulsion and by joint Grant 2016627 of the United States−Israel Binational Science Foundation (BSF), Jerusalem, Israel, and United States National Science Foundation (NSF) is acknowledged.

■ REFERENCES

(1) Crittenden, J. C.; Trussell; Hand, D. W.; Howe, K. J.; Tchobanoglous, G. *MWH's Water Treatment: Principles and Design*, Third ed.; John Wiley and Sons, 2012.

(2) Lee, K. P.; Arnot, T. C.; Mattia, D. A review of reverse osmosis membrane materials for desalination—Development to date and future potential. *J. Membr. Sci.* **2011**, *370* (1), 1−22.

(3) Shultz, S.; Bass, M.; Semiat, R.; Freger, V. Modification of polyamide membranes by hydrophobic molecular plugs for improved boron rejection. *J. Membr. Sci.* **2018**, *546*, 165−172.

(4) Levchenko, S.; Freger, V. Breaking the Symmetry: Mitigating Scaling in Tertiary Treatment of Waste Effluents Using a Positively Charged Nanofiltration Membrane. *Environ. Sci. Technol. Lett.* **2016**, *3* (9), 339−343.

(5) Hussain, A. A.; Nataraj, S. K.; Abashar, M. E. E.; Al-Mutaz, I. S.; Aminabhavi, T. M. Prediction of physical properties of nanofiltration membranes using experiment and theoretical models. *J. Membr. Sci.* **2008**, *310* (1−2), 321−336.

(6) Fievet, P. Donnan Steric Pore (DSP) and Dielectric Exclusion (DE) Model. In *Encyclopedia of Membranes*; Drioli, E., Giorno, L., Eds.; Springer: Berlin, Heidelberg, 2015; pp 1−5.

(7) Kotrappanavar, N. S.; Hussain, A. A.; Abashar, M. E. E.; Al-Mutaz, I. S.; Aminabhavi, T. M.; Nadagouda, M. N. Prediction of physical properties of nanofiltration membranes for neutral and charged solutes. *Desalination* **2011**, *280* (1), 174−182.

(8) Szymczyk, A.; Fievet, P. Investigating transport properties of nanofiltration membranes by means of a steric, electric and dielectric exclusion model. *J. Membr. Sci.* **2005**, *252* (1), 77−88.

(9) Nir, O.; Bishop, N. F.; Lahav, O.; Freger, V. Modeling pH variation in reverse osmosis. *Water Res.* **2015**, *87*, 328−335.
(10) Bason, S.; Freger, V. Phenomenological analysis of transport of mono- and divalent ions in nanofiltration. *J. Membr. Sci.* **2010**, *360* (1), 389−396.
(11) Xu, Y.; Lebrun, R. E. Investigation of the solute separation by charged nanofiltration membrane: effect of pH, ionic strength and solute type. *J. Membr. Sci.* **1999**, *158* (1), 93−104.
(12) Freger, V. Selectivity and polarization in water channel membranes: lessons learned from polymeric membranes and CNTs. *Faraday Discuss.* **2018**, *209*, 371−378.
(13) Freger, V. Ion partitioning and permeation in charged low-T* membranes. *Adv. Colloid Interface Sci.* **2020**, *277*, 102107.
(14) Ilani, A. The development of pressure across membranes in Donnan systems. *Sci. Rep.* **2015**, *5*, 14695.
(15) Mafé, S.; Manzanares, J. A.; Reiss, H. Donnan phenomena in membranes with charge due to ion adsorption. Effects of the interaction between adsorbed charged groups. *J. Chem. Phys.* **1993**, *98* (3), 2325−2331.
(16) Chen, D.; Werber, J. R.; Zhao, X.; Elimelech, M. A facile method to quantify the carboxyl group areal density in the active layer of polyamide thin-film composite membranes. *J. Membr. Sci.* **2017**, *534*, 100−108.
(17) Coronell, O.; Mariñas, B. J.; Zhang, X.; Cahill, D. G. Quantification of Functional Groups and Modeling of Their Ionization Behavior in the Active Layer of FT30 Reverse Osmosis Membrane. *Environ. Sci. Technol.* **2008**, *42* (14), 5260−5266.
(18) Coronell, O.; González, M. I.; Mariñas, B. J.; Cahill, D. G. Ionization Behavior, Stoichiometry of Association, and Accessibility of Functional Groups in the Active Layers of Reverse Osmosis and Nanofiltration Membranes. *Environ. Sci. Technol.* **2010**, *44* (17), 6808−6814.
(19) Perry, L. A.; Coronell, O. Reliable, bench-top measurements of charge density in the active layers of thin-film composite and nanocomposite membranes using quartz crystal microbalance technology. *J. Membr. Sci.* **2013**, *429*, 23−33.
(20) Tiraferri, A.; Elimelech, M. Direct quantification of negatively charged functional groups on membrane surfaces. *J. Membr. Sci.* **2012**, *389*, 499−508.
(21) Tang, C. Y.; Kwon, Y.-N.; Leckie, J. O. Probing the nano- and micro-scales of reverse osmosis membranes—A comprehensive characterization of physiochemical properties of uncoated and coated membranes by XPS, TEM, ATR-FTIR, and streaming potential measurements. *J. Membr. Sci.* **2007**, *287* (1), 146−156.
(22) Childress, A. E.; Elimelech, M. Relating Nanofiltration Membrane Performance to Membrane Charge (Electrokinetic) Characteristics. *Environ. Sci. Technol.* **2000**, *34* (17), 3710−3716.
(23) Childress, A. E.; Elimelech, M. Effect of solution chemistry on the surface charge of polymeric reverse osmosis and nanofiltration membranes. *J. Membr. Sci.* **1996**, *119* (2), 253−268.
(24) Hurwitz, G.; Guillen, G. R.; Hoek, E. M. V. Probing Polyamide Membrane Surface Charge, Zeta Potential, Wettability, and Hydrophilicity with Contact Angle Measurements. *J. Membr. Sci.* **2010**, *349* (1), 349−357.
(25) Shaffer, D. L.; Feldman, K. E.; Chan, E. P.; Stafford, G. R.; Stafford, C. M. Characterizing salt permeability in polyamide desalination membranes using electrochemical impedance spectroscopy. *J. Membr. Sci.* **2019**, *583*, 248−257.
(26) Liu, J.; Chen, Z.; Yao, L.; Wang, S.; Huang, L.; Dong, C.; Niu, L. The 2D platelet confinement effect on the membrane hole structure probed by electrochemical impedance spectroscopy. *Electrochem. Commun.* **2019**, *106*, 106517.
(27) Stolov, M.; Freger, V. Degradation of Polyamide Membranes Exposed to Chlorine: An Impedance Spectroscopy Study. *Environ. Sci. Technol.* **2019**, *53* (5), 2618−2625.
(28) Drazevic, E.; Bason, S.; Kosutic, K.; Freger, V. Enhanced Partitioning and Transport of Phenolic Micropollutants within Polyamide Composite Membranes. *Environ. Sci. Technol.* **2012**, *46* (6), 3377−3383.
(29) Fridman-Bishop, N.; Freger, V. When Salt-Rejecting Polymers Meet Protons: An Electrochemical Impedance Spectroscopy Investigation. *Langmuir* **2017**, *33* (6), 1391−1397.
(30) Freger, V.; Bason, S. Characterization of Ion Transport in Thin Films Using Electrochemical Impedance Spectroscopy: I. Principles and Theory. *J. Membr. Sci.* **2007**, *302* (1), 1−9.
(31) Karan, S.; Jiang, Z.; Livingston, A. G. Sub-10 nm Polyamide Nanofilms with Ultrafast Solvent Transport for Molecular Separation. *Science* **2015**, *348*, 1347.
(32) Bason, S.; Oren, Y.; Freger, V. Ion transport in the polyamide layer of RO membranes: composite membranes and free-standing films. *J. Membr. Sci.* **2011**, *367* (1), 119−126.
(33) Drazevic, E.; Bason, S.; Kosutic, K.; Freger, V. Enhanced Partitioning and Transport of Phenolic Micropollutants within Polyamide Composite Membranes. *Environ. Sci. Technol.* **2012**, *46* (6), 3377−3383.
(34) Pacheco, F. A.; Pinnau, I.; Reinhard, M.; Leckie, J. O. Characterization of isolated polyamide thin films of RO and NF membranes using novel TEM techniques. *J. Membr. Sci.* **2010**, *358* (1−2), 51−59.
(35) Bason, S.; Kedem, O.; Freger, V. Determination of concentration-dependent transport coefficients in nanofiltration: Experimental evaluation of coefficients. *J. Membr. Sci.* **2009**, *326* (1), 197−204.
(36) Bason, S.; Kaufman, Y.; Freger, V. Analysis of Ion Transport in Nanofiltration Using Phenomenological Coefficients and Structural Characteristics. *J. Phys. Chem. B* **2010**, *114* (10), 3510−3517.
(37) Strathmann, H. *Ion-Exchange Membrane Separation Processes*; Elsevier, 2004.
(38) Yeager, H. L.; Gronowski, A. A. Membrane Applications. In *Ionomers: Synthesis, Structure, Properties and Applications*; Tant, M. R.; Mauritz, K. A.; Wilkes, G. L., Eds. Springer, Netherlands; 1997; pp 333−364.
(39) Fridman-Bishop, N.; Freger, V. What makes aromatic polyamide membranes superior: New insights into ion transport and membrane structure. *J. Membr. Sci.* **2017**, *540*, 120−128.
(40) Dražević, E.; Košutić, K.; Freger, V. Permeability and Selectivity of Reverse Osmosis Membranes: Correlation to Swelling Revisited. *Water Res.* **2014**, *49*, 444−452.
(41) La, Y.-H.; Sooriyakumaran, R.; Miller, D. C.; Fujiwara, M.; Terui, Y.; Yamanaka, K.; McCloskey, B. D.; Freeman, B. D.; Allen, R. D. Novel thin film composite membrane containing ionizable hydrophobes: pH-dependent reverse osmosis behavior and improved chlorine resistance. *J. Mater. Chem.* **2010**, *20* (22), 4615−4620.
(42) Cadotte, J. E.; Petersen, R. J.; Larson, R. E.; Erickson, E. E. A new thin-film composite seawater reverse osmosis membrane. *Desalination* **1980**, *32*, 25−31.
(43) Mänttäri, M.; Pihlajamäki, A.; Nyström, M. Effect of pH on hydrophilicity and charge and their effect on the filtration efficiency of NF membranes at different pH. *J. Membr. Sci.* **2006**, *280* (1), 311−320.
(44) Nilsson, M.; Tragardh, G.; Ostergren, K. The influence of pH, salt and temperature on nanofiltration performance. *J. Membr. Sci.* **2008**, *312* (1−2), 97−106.
(45) Freger, V.; Arnot, T. C.; Howell, J. A. Separation of concentrated organic/inorganic salt mixtures by nanofiltration. *J. Membr. Sci.* **2000**, *178* (1−2), 185−193.
(46) Freger, V. Swelling and Morphology of the Skin Layer of Polyamide Composite Membranes: An Atomic Force Microscopy Study. *Environ. Sci. Technol.* **2004**, *38* (11), 3168−3175.
(47) Zhang, X. J.; Cahill, D. G.; Coronell, O.; Marinas, B. J. Absorption of water in the active layer of reverse osmosis membranes. *J. Membr. Sci.* **2009**, *331* (1−2), 143−151.
(48) Kolev, V.; Freger, V. Hydration, porosity and water dynamics in the polyamide layer of reverse osmosis membranes: A molecular dynamics study. *Polymer* **2014**, *55* (6), 1420−1426.
(49) Dražević, E.; Košutić, K.; Freger, V. Permeability and selectivity of reverse osmosis membranes: Correlation to swelling revisited. *Water Res.* **2014**, *49* (0), 444−452.

https://dx.doi.org/10.1021/acs.estlett.0c00291
Environ. Sci. Technol. Lett. 2020, 7, 440−445

(50) Bason, S.; Oren, Y.; Freger, V. Characterization of Ion Transport in Thin Films Using Electrochemical Impedance Spectroscopy: II: Examination of the Polyamide Layer of RO Membranes. *J. Membr. Sci.* **2007**, *302* (1), 10−19.
(51) Lanteri, Y.; Fievet, P.; Szymczyk, A. Evaluation of the steric, electric, and dielectric exclusion model on the basis of salt rejection rate and membrane potential measurements. *J. Colloid Interface Sci.* **2009**, *331* (1), 148−155.

https://dx.doi.org/10.1021/acs.estlett.0c00291
Environ. Sci. Technol. Lett. 2020, 7, 440−445